VIP Metal-Ion Batteries Very Important Paper

International Edition: DOI: 10.1002/anie.201803703
German Edition: DOI: 10.1002/ange.201803703

A Universal Organic Cathode for Ultrafast Lithium and Multivalent Metal Batteries

*Xiulin Fan[+], Fei Wang[+], Xiao Ji, Ruixing Wang, Tao Gao, Singyuk Hou, Ji Chen, Tao Deng, Xiaogang Li, Long Chen, Chao Luo, Luning Wang, and Chunsheng Wang**

Abstract: *Low-cost multivalent battery chemistries (Mg^{2+}, Al^{3+}) have been extensively investigated for large-scale energy storage applications. However, their commercialization is plagued by the poor power density and cycle life of cathodes. A universal polyimides@CNT (PI@CNT) cathode is now presented that can reversibly store various cations with different valences (Li^+, Mg^{2+}, Al^{3+}) at an extremely fast rate. The ion-coordination charge storage mechanism of PI@CNT is systemically investigated. Full cells using PI@CNT cathodes and corresponding metal anodes exhibit long cycle life (>10000 cycles), fast kinetics (>20 C), and wide operating temperature range (−40 to 50°C), making the low-cost industrial polyimides universal cathodes for different multivalent metal batteries. The stable ion-coordinated mechanism opens a new foundation for the development of high-energy and high-power multivalent batteries.*

The present energy-storage landscape has been dominated by lithium ion batteries (LIBs) since the first commercialization in 1991 because of their high energy density.[1] However, numerous safety incidents, limited resource supplies (lithium, cobalt), and high costs seem to constrain the large-scale utilization on the automotive market and in stationary energy storage systems.[2] The increasing demand for the integration of intermittent electricity generated from renewable energies (such as solar and wind) into the grid calls for beyond Li-ion batteries that are environmentally friendly/benign, safe, cost-efficient, and have a long cycle life.[3] Among the battery chemistries beyond the Li-ion,[4] magnesium metal batteries (MMBs)[5] and aluminum metal batteries (AMBs)[6] are promising for large scale energy storage because the Mg and Al metals are not only abundant and safe to handle in ambient atmosphere, but also energetically conferred by the multi-electron redox.[2,5a,6,7] The specific capacity and reduction potentials of Li, Na, Mg, and Al are compared n the Supporting Information, Table S1. Mg and Al metals have a relatively high negative reduction potential (−2.4 V and −1.7 V versus NHE, respectively), and the highest volumetric capacities (3833 and 8046 $mAh\,cm^{-3}$, respectively). For the Mg and Al batteries, another important merit is the potentially dendrite-free deposition owing to their relatively higher Mg–Mg or Al–Al bond energies compared with Li–Li bond.[8] All of these features render Mg and Al metal rechargeable batteries compelling candidates for sustainable electrochemical storage devices at both large and intermediate scales.[9] However, the cell performances of these multivalent batteries are impeded by low power density owing to the intrinsic low ion diffusion rate of multivalent ions in the solid state cathode materials, short cycling life owing to the poor reversibility, and low round-trip efficiency that is due to large voltage hysteresis between charge and discharge.[9c,d,5b,10] The electrochemical intercalation of these multivalent cations into a host crystal structure is difficult due to the strong electrostatic interaction between the cations and the host lattices, which restricts the redistribution of the electric charges of the cations. The diffusion barriers of these multivalent ions are orders of magnitude higher than that of Li^+ ions in the same host matrix, limiting the rate capability (power), or even preventing the insertion of these ions.[11] Sulfur and selenium have lower electronegativity than oxygen and are more polarizable owing to their large atom radius. Therefore, the charge redistribution in the sulfide or selenium anionic frameworks shows superior to their corresponding oxides due to the softer lattices.[10b,12] To date, the Chevrel phase Mo_6S_8 is still the prototype intercalation cathode with high cycling stability for Mg^{2+} and Al^{3+} due to its special crystal structure, which is the milestones for the Mg^{2+} and Al^{3+} batteries.[5a,9d]

Herein, we report that industrial polyimide (PI) polymer is a universal cathode materials for Li^+, Mg^{2+}, and Al^{3+}, and these metal/PI batteries have very high power density and long cycle life. Detail electrochemical, spectroscopic, and microscopy characterization revealed that Li^+, Mg^{2+}, and Al^{3+} intercalate into PI polymer through a stable ion-coordination charge storage mechanism, which is totally different from the conventional inorganic materials, and is the key reason for the superior power density of the multi-valent batteries. Since the structurally stable ion-coordination charge storage mechanism allows fast cation diffusion in the PI@CNT cathode materials, we bypassed the traditional obstacles of slow kinetics, large voltage hysteresis, and low reversibility for the multivalent batteries. Therefore, this new type of elec-

[*] Dr. X. Fan,[+] Dr. X. Ji, Dr. T. Gao, S. Hou, Dr. J. Chen, T. Deng, Dr. X. Li, Dr. L. Chen, Dr. C. Luo, Prof. C. Wang
Department of Chemical and Biomolecular Engineering
University of Maryland, College Park, MD 20742 (USA)
E-mail: cswang@umd.edu
Dr. F. Wang[+]
Electrochemistry Branch, Sensor and Electron Devices Directorate
Power and Energy Division U.S. Army Research Laboratory
Adelphi, MD 20783 (USA)
R. Wang, L. Wang
Department of Chemistry and Biochemistry, University of Maryland
College Park, MD 20742 (USA)
[+] These authors contributed equally to this work.
Supporting information and the ORCID identification number(s) for the author(s) of this article can be found under: https://doi.org/10.1002/anie.201803703.

trode materials enables the low-cost MMBs and AMBs to achieve extremely long cycle life and high power density (fast kinetics) as that of LIBs.

The preparation process of the PI/CNT composite is shown in Figure 1 a, with a detailed experimental description given in the Supporting Information. The as-purchased CNT was first pre-treated to ensure the homogeneously dispersion

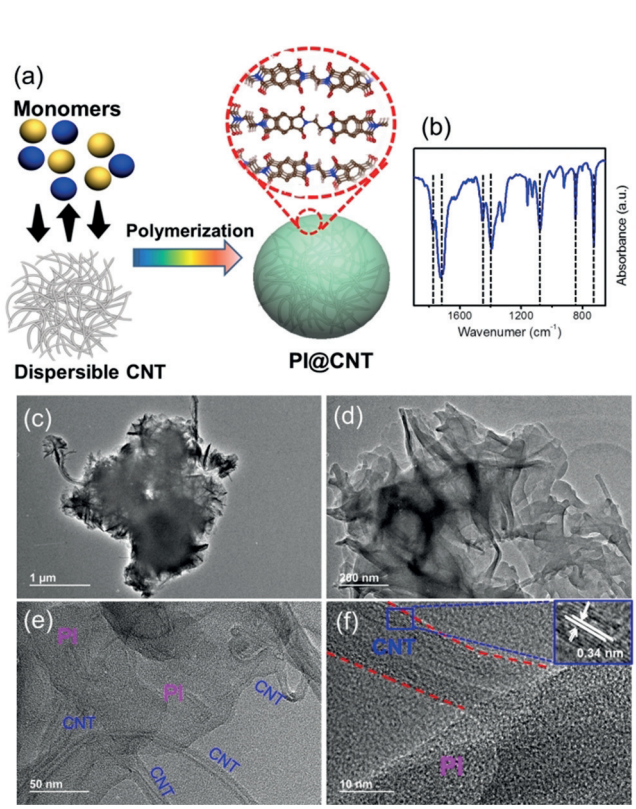

Figure 1. a) Illustration of PI@CNT synthesis. b) FTIR spectra of the as-synthesized PI@CNT. TEM images (c, d, e) and HRTEM image (f) of the PI/CNT composite. PI and carbon nanotubes (CNT) are marked according to the crystal features of the carbon nanotubes.

in the NMP solvent. SEM images of the dispersive carbon nanotubes are shown in the Supporting Information, Figure S1a,b. At low magnification, these CNTs present an irregular shape with tens of micrometers (Supporting Information, Figure S1a). Under high magnification, individual CNTs can be observed, and these CNTs are loosely entangled with empty space between them (Supporting Information, Figure S1b). These dispersible CNTs contact with each other to form a network. The dispersed CNT in NMP can keep for over 1 week without any deposit (Supporting Information, Figure S1c,d). Figure 1 b shows the FTIR spectrum of the PI@CNT, which is in agreement with the previous report.[13] Figure 1 c–e show the TEM images of the PI@CNT composite. After polymerization of the PI, distinct carbon nanotubes can be clearly detected in the composite, in which the carbon nanotubes linked these PI nanoparticles into micrometers (Supporting Information, Figure S2), implying that the PI formed in situ is filled into the empty space between the carbon nanotubes, suggesting a good tap density. This hierarchical structure can ensure a high electronic conductivity for the composite, which is a pre-requisite for the high kinetics of the electrodes. As shown by the high resolution TEM image in Figure 1 f, the graphitic layers in CNT can be observed. These long CNTs are randomly distributed in the composite, and connected different domains of PI together, forming effective conductive networks (Figure 2 d,e).

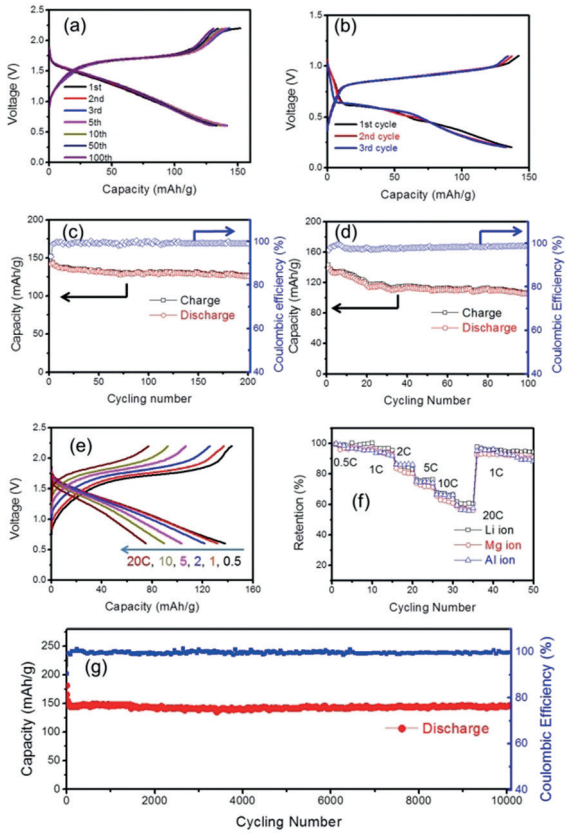

Figure 2. Electrochemical performance of the PI@CNT cathode for different metal batteries. a) Galvanostatic charge-discharge voltage profiles of PI@CNT as Mg-ion cathode at a current density of 1 C (1 C = 150 mA g^{-1}); b) Galvanostatic charge–discharge voltage profiles of PI@CNT as Al-ion cathode at a current density of 1 C (1 C = 150 mA g^{-1}); c) Cycling performance of PI@CNT as Mg-ion cathode; d) Cycling performance of PI@CNT as Al-ion cathode; e) Voltage profiles of PI@CNT composite as Mg-ion cathode at different current densities; f) Comparison of rate performance of PI@CNT composite as Li, Mg, and Al ion cathodes. (g) Cycling performance of PI@CNT as Li ion cathode at a current of 10 C in the electrolyte of 4 M LiFSI DME.

Polyimide was investigated as a cathode material for the Li ion batteries.[13] However, the reaction rate is slow for practical application owing to the low electron conductivity of polyimide. We tackled this issue by in situ formation of a PI@CNT composite, in which the CNTs are connected with each other to construct a 3D electron conductive matrix. show the electrochemical performance of the PI@CNT cathodes for Li^+, Mg^{2+}, and Al^{3+} batteries are shown in Figure 2 and the Supporting Information, Figure S3. Both capacity and current density are calculated based on the overall weight of the PI@CNT composite. The PI@CNT cathodes provide a highly reversible capacity of 180 mAh g^{-1}, circa 130 mAh g^{-1}, and

110 mAh g^{-1} for Li, Mg, and Al ion batteries (Supporting Information, Figure S3; Figure 2a and b), respectively. It should be mentioned that the PI@CNT can also reversibly store the Na ions with a high capacity of about 150 mAh g^{-1}, and possess a good cycling stability (Supporting Information, Figure S4). Such stable cycle performance for the MMBs or AMBs has rarely been reported. The energy densities of the Mg and Al batteries are lower compared with the Li battery owing to the relatively low voltage (Figure 2a,b). However, considering the intrinsically dendritic suppression of the Mg and Al metal anodes (Supporting Information, Figures S5, S6), the Mg and Al batteries can still be utilized as promising large-scale energy storage technologies. The cycle life of PI@CNT cathodes can be further enhanced by tuning the electrolytes. As the electrolyte was changed to 4 M LiFSI DME electrolyte, no capacity decay was observed even after 10000 cycles (Figure 2g) for the LIB. This reversibility improvement could be due to the totally suppression of the possible dissolution of the organic polymers in the concentrated electrolyte. Along with the long cycling stability, the more striking feature for PI@CNT cathode is the supper rate capabilities for Mg^{2+} and Al^{3+} insertion/extraction (Figure 2e,f), which is totally different from the sluggish kinetics observed for the multivalent ion insertion into the inorganic materials.[10b,14] As the charge–discharge current increases to 3 A g^{-1} (20 C), the PI@CNT still retains 55% of the reversible capacity at 0.5 C for all Li^+, Mg^{2+}, and Al^{3+} reactions (Figure 2e,f). More interestingly, the PI@CNT composite can even maintain the high rate capability and long cycling stability at a low temperature for all three ion batteries. At −40 °C, PI@CNT can still deliver a reversible capacity of 65 mAh g^{-1} and maintain 100 cycle life at −20 °C for the MMBs (Supporting Information, Figure S7). The excellent cyclability, high rate capability, and superior low-temperature kinetics suggest ion insertion into in PI@CNT through a different ion storage mechanism compared to the previously reported inorganic crystal materials.[10b,15]

The mechanism for the fast reaction kinetics of the PI polymers in different batteries was investigated using cyclic voltammetry (CV) at different sweep rates from 0.05 to 1.0 mV s^{-1}. All the CV curves for Li^+, Mg^{2+}, and Al^{3+} exhibit similar shapes with a pair of broaden peaks in cathodic and anodic processes (Supporting Information, Figure S8). Detail analysis revealed that the broad cathodic and anodic peaks of PI@CNT composite for Li^+, Mg^{2+}, and Al^{3+} batteries show a mainly pseudo-capacitive behavior. The stepwise increase of the scan rate from 0.05 to 1 mV s^{-1} shows only a small increase in polarization, which in principle demonstrates the inherently fast kinetics of the intercalation of different ions into PI@CNT composite, and is in good agreement with the fast rate capability (Figure 2f).

For an ion storage reaction, the measured current (i) at a fixed potential obeys a power-law relationship with the potential sweep rate (v) [Eq. (1)]. To quantitatively determine the contribution of capacitive reaction and diffusion reaction on the capacity of PI@CNT cathodes, the voltammetric responses of PI@CNT at various sweep rates were analyze using Equation (1):[16]

$$i = a v^b \quad (1)$$

For a redox reaction limited by semi-infinite diffusion, the peak current i varies with $v^{1/2}$ (that is, $b = 0.5$); for a capacitive process, it varies with v (that is, $b = 1$). Figure 3a shows the plots of log(i) versus log(v) of the peak current responses. In our experiments, the PI@CNT composite exhibits values of b approximately between 0.75–0.85 for different valent batteries (Figure 3a), implying that a significant portion of the M^{n+} intercalation capacity has surface-controlled characteristics, which endows PI@CNT composite a supercapacitor-like electrochemical behavior.

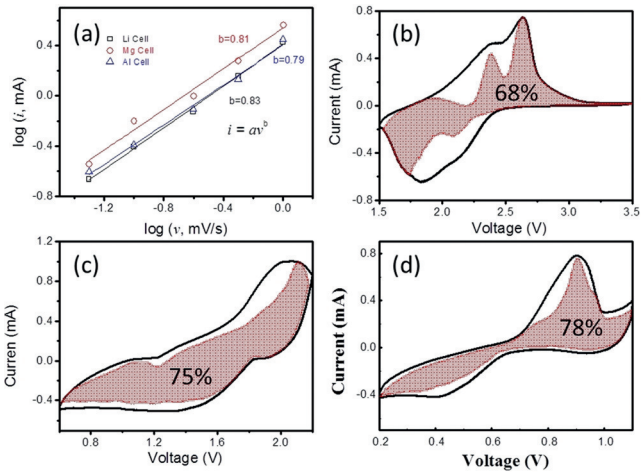

Figure 3. Kinetics and quantitative mechanism analysis of different valent batteries. a) Determination of b values using the relationship between peak current and scanning rate. Capacitive (red area) and diffusion-controlled contribution to charge storage of PI/CNT composite at 0.25 mV s^{-1} for different valent batteries: b) LIBs; c) MMBs; d) AMBs.

Further analysis determines the level of this surface control reaction contribution by using the relation of current response, i, with a combination of capacitor-like (proportional to the scan rate v) and diffusion-controlled behaviors ($k_2 v^{1/2}$), according to Dunn et al. [Equation (2)]:[17]

$$i = k_1 v + k_2 v^{1/2} \quad (2)$$

By determining both k_1 and k_2 constants, we can distinguish the fraction of the current from surface capacitance and M^{n+} semi-infinite linear diffusion. Figure 3b–d show the typical voltage profiles for capacitive current (red region) in comparison with the total current for the Li^+, Mg^{2+}, and Al^{3+} cells. At a slow scanning rate of 0.25 mV s^{-1}, the surface-control contribution is 68%, 75%, and 78% for the Li^+, Mg^{2+}, and Al^{3+} storage, respectively. Therefore, the high power density for the PI polymer cathode for different valent ions was enabled by the unique structure of the active sites that effectively shortens the M^{n+} diffusing distances and accelerates the redox reactions.

The surface-dominated pseudocapacitance is identified as a major energy-storage mechanism for the PI@CNT compo-

site enabling high-rate capacity. The detailed ion-storage mechanism of PI@CNT was also theoretically analyzed. First, the chemically bonded PI@CNT hybrid has excellent structure stability (Supporting Information, Figures S9–S12) and has high electronic/ionic conductivity throughout the network, which are prerequisite for the extrinsic pseudocapacitance, as demonstrated in nanosized MoO_3 and SnS.[17b,19] Secondly, the nanoscale dimension with the soft structure of the PI also promotes the fast diffusion of the solvated ions and corresponding redox capacitive contribution. During transfer of ions and electrons, the solvated cations can easily enter into the open spaces between neighboring active sites in the polymer, while the electrons can fast migrate on the skeleton of the carbon nanotubes.

In contrast to the slow solid-state ion diffusion and phase transformation in inorganic materials with stiff crystal structure,[18] the present soft structure of PI@CNT composite with a pseudocapacitive-like behavior offers an opportunity to enhance the reaction kinetics and cycling stability even for high-valence ions, revolutionizing the traditional low-power and poor cycle life multivalent battery chemistries.

The reduction potentials and mechanism for pseudocapacitive-like behavior of the PI for Li-PI and Mg-PI were also theoretical analyzed. Detailed calculations are shown in supporting information (Supporting Information, Figure S13). According to the calculations, Li ions and the solvated Mg ions will readily bond with the carbonyl group in the PI polymers during the discharge process. The calculated reduction potentials are well consistent with the charge–discharge voltages in Figure 2. The results also indicated that Mg tend to react with PI with the form of $Mg(THF)_2Cl$. The solvated solvent molecules could effectively shield the strong electrostatic interactions between the cations and the host structure. The flexible structure of $Mg(THF)_2Cl$ can accommodate the host structure better and benefit the kinetics. Moreover, the weak van der Waals interactions between the chains in PI provide an ideal host for these cations. As a consequence, similar to supercapacitors, the limiting factor for high rate charge–discharge is the transfer of ions and electrons to the active sites in the PI polymer rather than the conventional solid-state diffusions, which makes PI a promising electrode material for fast charge and discharge battery. Figure 4b demonstrated that two Swagelok-type Mg/PI cells power 50 light-emitting diode (LED) bulbs.

In conclusion, we show that polyimides are suitable as a universal cathode for different multivalent batteries (Li^+, Mg^{2+}, Al^{3+}), allowing fast multivalent insertion/extraction through viable ion-coordination charge storage mechanism, which is totally different from the inorganic materials. PI@CNT cathodes show high Coulombic efficiency, long cycle life, and fast kinetics for Mg^{2+} and Al^{3+}, rendering them promising contenders for large-scale energy storage. Furthermore, the organic polymers resolve serious kinetics and cost concerns of the previous multivalent battery chemistries using inorganic crystalline cathode materials. The present work provides a new opportunity to design the high power and long cycle life multivalent rechargeable batteries.

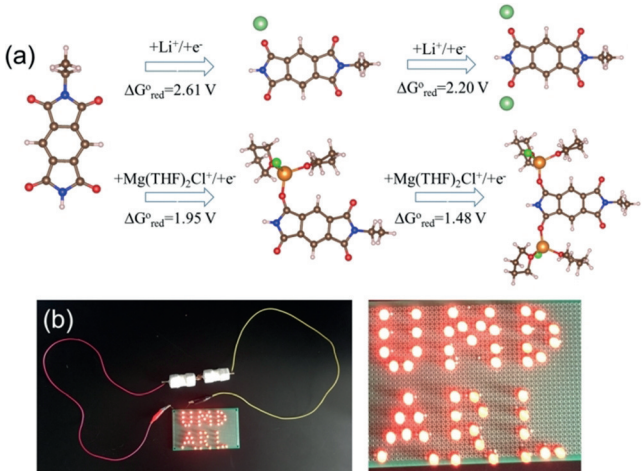

Figure 4. a) Reduction potentials and corresponding complexes obtained from quantum chemistry (QC) calculations for Li-PI and Mg-PI systems. b) The application of MMBs, powering 50 LED bulbs.

Acknowledgements

This work was supported as part of the Nanostructures for Electrical Energy Storage (NEES), an Energy Frontier Research Center funded by the U.S. Department of Energy, Office of Science, Basic Energy Sciences under Award number DESC0001160. We acknowledge the support of the Maryland NanoCenter and the US National Science Foundation Award 1438198.

Conflict of interest

The authors declare no conflict of interest.

Keywords: aluminum · lithium ion batteries · magnesium · multivalent batteries · organic cathodes

How to cite: *Angew. Chem. Int. Ed.* **2018**, *57*, 7146–7150
Angew. Chem. **2018**, *130*, 7264–7268

[1] A. Yoshino, *Angew. Chem. Int. Ed.* **2012**, *51*, 5798–5800; *Angew. Chem.* **2012**, *124*, 5898–5900.
[2] J. F. Parker, C. N. Chervin, I. R. Pala, M. Machler, M. F. Burz, J. W. Long, D. R. Rolison, *Science* **2017**, *356*, 415–418.
[3] a) D. Larcher, J. M. Tarascon, *Nat. Chem.* **2015**, *7*, 19–29; b) T. Janoschka, N. Martin, U. Martin, C. Friebe, S. Morgenstern, H. Hiller, M. D. Hager, U. S. Schubert, *Nature* **2015**, *527*, 78–81.
[4] a) H. Pan, Y.-S. Hu, L. Chen, *Energy Environ. Sci.* **2013**, *6*, 2338–2360; b) N. Yabuuchi, K. Kubota, M. Dahbi, S. Komaba, *Chem. Rev.* **2014**, *114*, 11636–11682.
[5] a) D. Aurbach, Z. Lu, A. Schechter, Y. Gofer, H. Gizbar, R. Turgeman, Y. Cohen, M. Moshkovich, E. Levi, *Nature* **2000**, *407*, 724–727; b) P. Canepa, G. Sai Gautam, D. C. Hannah, R. Malik, M. Liu, K. G. Gallagher, K. A. Persson, G. Ceder, *Chem. Rev.* **2017**, *117*, 4287–4341; c) X. Miao, Z. Chen, N. Wang, Y. Nuli, J. Wang, J. Yang, S.-i. Hirano, *Nano Energy* **2017**, *34*, 26–35.
[6] M.-C. Lin, M. Gong, B. Lu, Y. Wu, D.-Y. Wang, M. Guan, M. Angell, C. Chen, J. Yang, B.-J. Hwang, H. Dai, *Nature* **2015**, *520*, 324–328.
[7] a) T. Ouchi, H. Kim, B. L. Spatocco, D. R. Sadoway, *Nat. Commun.* **2016**, *7*, 10999; b) J. Fu, Z. P. Cano, M. G. Park, A.

Yu, M. Fowler, Z. Chen, *Adv. Mater.* **2017**, *29*, 1604685; c) C. P. Grey, J. M. Tarascon, *Nat. Mater.* **2017**, *16*, 45 – 56; d) L. Chen, J. L. Bao, X. Dong, D. G. Truhlar, Y. Wang, C. Wang, Y. Xia, *ACS Energy Lett.* **2017**, *2*, 1115 – 1121; e) F. Wang, X. Fan, T. Gao, W. Sun, Z. Ma, C. Yang, F. Han, K. Xu, C. Wang, *ACS Cent. Sci.* **2017**, *3*, 1121 – 1128.

[8] Y. Lu, Z. Tu, L. A. Archer, *Nat. Mater.* **2014**, *13*, 961 – 969.

[9] a) N. Jayaprakash, S. K. Das, L. A. Archer, *Chem. Commun.* **2011**, *47*, 12610 – 12612; b) Z. Li, K. Xiang, W. Xing, W. C. Carter, Y.-M. Chiang, *Adv. Energy Mater.* **2015**, *5*, 1401410; c) M. M. Huie, D. C. Bock, E. S. Takeuchi, A. C. Marschilok, K. J. Takeuchi, *Coord. Chem. Rev.* **2015**, *287*, 15 – 27; d) L. Geng, G. Lv, X. Xing, J. Guo, *Chem. Mater.* **2015**, *27*, 4926 – 4929.

[10] a) E. Levi, Y. Gofer, D. Aurbach, *Chem. Mater.* **2010**, *22*, 860 – 868; b) X. Sun, P. Bonnick, L. F. Nazar, *ACS Energy Lett.* **2016**, *1*, 297 – 301.

[11] C. Ling, F. Mizuno, *Chem. Mater.* **2013**, *25*, 3062 – 3071.

[12] X. Sun, P. Bonnick, V. Duffort, M. Liu, Z. Rong, K. A. Persson, G. Ceder, L. F. Nazar, *Energy Environ. Sci.* **2016**, *9*, 2273 – 2277.

[13] Z. Song, H. Zhan, Y. Zhou, *Angew. Chem. Int. Ed.* **2010**, *49*, 8444 – 8448; *Angew. Chem.* **2010**, *122*, 8622 – 8626.

[14] T. Kouji, G. Yunpeng, K. Yukari, Y. Takafumi, T. Hidenori, *Appl. Phys. Express* **2016**, *9*, 011801.

[15] Z. Tao, L. Xu, X. Gou, J. Chen, H. Yuan, *Chem. Commun.* **2004**, 2080 – 2081.

[16] a) X. Dong, L. Chen, J. Liu, S. Haller, Y. Wang, Y. Xia, *Sci. Adv.* **2016**, *2*, e1501038; b) Y. Wang, X. Cui, Y. Zhang, L. Zhang, X. Gong, G. Zheng, *Adv. Mater.* **2016**, *28*, 7626 – 7632.

[17] a) T. Brezesinski, J. Wang, S. H. Tolbert, B. Dunn, *Nat. Mater.* **2010**, *9*, 146 – 151; b) H.-S. Kim, J. B. Cook, H. Lin, J. S. Ko, S. H. Tolbert, V. Ozolins, B. Dunn, *Nat. Mater.* **2017**, *16*, 454 – 460.

[18] a) T. Gao, X. Li, X. Wang, J. Hu, F. Han, X. Fan, L. Suo, A. J. Pearse, S. B. Lee, G. W. Rubloff, K. J. Gaskell, M. Noked, C. Wang, *Angew. Chem. Int. Ed.* **2016**, *55*, 9898 – 9901; *Angew. Chem.* **2016**, *128*, 10052 – 10055; b) T. Gao, M. Noked, A. J. Pearse, E. Gillette, X. Fan, Y. Zhu, C. Luo, L. Suo, M. A. Schroeder, K. Xu, S. B. Lee, G. W. Rubloff, C. Wang, *J. Am. Chem. Soc.* **2015**, *137*, 12388 – 12393.

[19] D. Chao, C. Zhu, P. Yang, X. Xia, J. Liu, J. Wang, X. Fan, S. V. Savilov, J. Lin, H. J. Fan, Z. X. Shen, *Nat. Commun.* **2016**, *7*, 12122.

Manuscript received: March 27, 2018
Accepted manuscript online: April 27, 2018
Version of record online: May 14, 2018

